

October 1993

 hep-ph/9312319
 SMU-HEP/93-17
 MSU-HEP 93/17
 PSU/TH/138

Leptoproduction of Heavy Quarks II

– A Unified QCD Formulation of Charged and Neutral Current Processes from Fixed-target to Collider Energies

M. A. G. Aivazis,^a John C. Collins,^b Fredrick I. Olness,^{a1} and Wu-Ki Tung^c

^aSouthern Methodist University, Dallas, Texas 75275

^bPenn State University, University Park, PA 16802

^cMichigan State University East Lansing, Michigan 48824

Abstract

A unified QCD formulation of leptoproduction of massive quarks in charged current and neutral current processes is described. This involves adopting consistent factorization and renormalization schemes which encompass both vector-boson-gluon-fusion (“flavor creation”) and vector-boson-massive-quark-scattering (“flavor excitation”) production mechanisms. It provides a framework which is valid from the threshold for producing the massive quark (where gluon-fusion is dominant) to the very high energy regime when the typical energy scale μ is much larger than the quark mass m_Q (where the quark-scattering should be prevalent). This approach effectively resums all large logarithms of the type $(\alpha_s(\mu) \log(\mu^2/m_Q^2))^n$ which limit the validity of existing fixed-order calculations to the region $\mu \sim O(m_Q)$. We show that the (massive) quark-scattering contribution (after subtraction of overlaps) is important in most parts of the (x, Q) plane except near the threshold region. We demonstrate that the factorization scale dependence of the structure functions calculated in this approach is substantially less than those obtained in the fixed-order calculations, as one would expect from a more consistent formulation.

PACS numbers: 12.38.Bx, 11.10.Gh, 13.60.Hb

¹SSC Fellow

1 Introduction

The production of heavy quarks in photo-, lepto-, and hadro-production processes has become an increasingly important subject of study from both the theoretical and experimental points of view. However, there are some outstanding problems with existing perturbative QCD calculations of heavy quark production: sizable (spurious) scale dependence of the predictions, apparent disagreement with observed b-production cross-section at the Tevatron, ... etc. See Ref.[1] for a recent review of the theory and phenomenology of heavy quark production. As will be discussed later in this paper, there is also an inconsistency in most theoretical calculations of the cross sections: the schemes used in the next-to-leading order calculations are not the same as those used in determining the parton densities from global analyses, such as in Refs. [2, 3, 4]. In this paper we will spell out the details of a more complete and consistent formulation of heavy quark production. For the sake of clarity, we shall focus on the case of lepto-production, although the same principles apply to hadroproduction as well.

Perturbative QCD calculations rely on factorization theorems^[6]: Different factors involve different scales of virtuality, and a factor that involves only physics on a scale m can be effectively calculated in a power series in $\alpha_s(m)$. The simplest factorizations, like the operator product expansion, are for certain two-scale problems: One scale, about the bound-state nature of hadrons, is of the order of Λ or the mass of a typical hadron; and the other, defining a scale of large virtuality, can be Q^2 in deep-inelastic scattering or the transverse momentum of a measured jet.²

Processes involving heavy quarks are a good example of a multi-scale process, for in practice we may then have to deal with at least four scales (which we denote by μ_i): Λ , Q^2 (as above), and the masses of the charm and bottom quarks, m_c and m_b . When one uses conventional calculational schemes designed for two-scale problems, the presence of more than one large scale results in logarithms $\ln(\mu_i/\mu_j)$ of the large ratios in the higher order correction terms. These logarithms vitiate the very basis of the original perturbative calculation, because of the large size of the yet higher order terms beyond the order included. In view of the high energies at present colliders, this problem can defeat the large effort put into existing fixed order calculations.^[1]

The basic principles for treating this situation were constructed a long time ago by Witten in his work^[7] on heavy quarks in the operator product expansion (OPE). But his methods as they stand do not provide a sufficient algorithm for calculating the processes in which we are interested. An important practical concern is that the methods of calculation should be applicable when some of the scales of interest are comparable to each other as well as when they are very different. Simple minded methods involving “integrating out the heavy quarks” are not sufficient, but, as Collins, Wilczek and Zee^[8] pointed out a long time ago, the problem can be conveniently considered as one of choice of the subtraction scheme (for renormalization and factorization). We shall refer to this work as CWZ in the following.

Consider the case of deep-inelastic scattering, with Q denoting the invariant mass of the

²To avoid circumlocutions, we will often use the terminology of the operator product expansion when discussing factorization theorems. In particular, we will use the term “Wilson coefficient” to denote the short-distance coefficient in the standard factorization theorem for deep inelastic scattering etc.

exchanged boson, and with one heavy quark, of mass m . Three kinematic regions are of interest:

- $m \gg Q$: The quark mass is larger than all other scales in the problem, so that the decoupling theorem^[9] applies: All graphs involving the heavy quark may be dropped, at the price only of a possible finite renormalization of the parameters of the theory, notably α_s .
- $m = O(Q)$: The heavy quark mass must be treated in the same way as Q — as a large parameter. Heavy quark lines appear in the Wilson coefficients or in finite renormalizations of exactly the same kind as in the decoupling theorem.
- $m \ll Q$: As far as the OPE is concerned, the heavy quark is to be treated as light: its mass is to be neglected in Wilson coefficients, and there are parton densities for the heavy quark. Since the quark is heavy on an absolute scale, *i.e.*, $m \gg \Lambda$, Witten’s methods may be used to calculate its density in terms of the densities of light partons.

The method we will describe will give a unified treatment that will cover all ranges of mass. Furthermore, the CWZ method also allows us to treat the case that there are several heavy quarks, whose masses may or may not be strongly ordered.

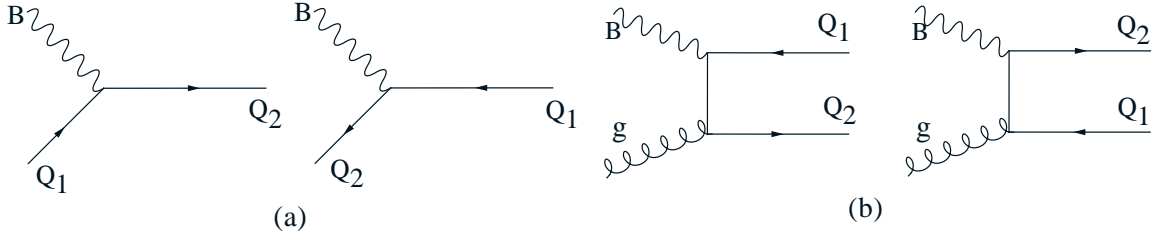


Figure 1: Amplitudes for heavy quark production: (a) order α_s^0 quark-scattering; and (b) order α_s^1 gluon-fusion contributions. At least one of the quarks, say Q_2 , is “heavy” and corresponds to the “Q” used in the text. For flavor changing currents, the two quarks Q_1 and Q_2 are different. For neutral currents, they are the same.

One can see the issues in contrasting treatments of heavy quark production in lepton-hadron scattering in existing literature.^[10] For charged current interactions, such as charm production in neutrino processes, most existing work focuses on the dominant underlying order- α_s^0 parton process $W + s \rightarrow c$ (*cf.* Fig. 1a, the quark-scattering or “flavor-excitation” sub-process).^[11, 12, 13, 14, 15, 16, 17] In contrast, for neutral current interactions, such as charm and bottom production in electron- and muon-hadron scattering, practically all calculations begin with the order- α_s^1 parton process $\gamma/Z^0 + g \rightarrow c + \bar{c}$ (*cf.* Fig. 1b, the gluon-fusion or “flavor-creation” sub-process).^[18, 19] In both cases the initiating parton is a light parton, and an appropriate scheme for computing radiative corrections is what we will call a 3-flavor scheme, where the heavy quark only occurs in the Wilson coefficients, and where there is no parton density for the charm and bottom quarks.

But at very high energies (such as are now available at the HERA $e - p$ collider and beyond) charm and bottom quark masses can become small compared to a typical energy

scale: we can have $Q^2 \gg m_c^2, m_b^2$. It is then natural to count these heavy quarks, especially the charm quark, as partons.[20, 21, 22, 23] We then effectively use a 4-flavor or 5-flavor scheme (as is done in commonly used parton distributions[2, 3, 4, 24]). In particular, the lowest order Wilson coefficient for charm production in the neutral current process is not gluon fusion, but flavor excitation $\gamma/Z^0 + c \rightarrow c$. Of course, the gluon density is rather large compared to the charm quark density, so that higher order gluon fusion process can be numerically comparable or larger than the flavor excitation process. (It is misleading to argue that an order α_s^1 subprocess is smaller than an order α_s^0 subprocess merely by virtue of its being higher order unless the initiating partons are the same.) Moreover, one must make the correct subtraction from the gluon fusion process to avoid double counting.

Evidently, for this purpose, the notion of a quark with mass m_Q being “heavy” or “light” must be taken as *relative* — with respect to the energy scale of the probe μ_{phy} . The latter view forms the very basis of the QCD parton model for the well-known light quarks u , d and s (which do have non-zero, albeit small, masses!). The parton approach effectively resums large logarithms in fixed-order calculations arising from initial state collinear singularities of the form $(\alpha_s \log \mu_{phy}/m_Q)^n$ to all orders in α_s .

On the other hand, one also has an *absolute* notion for the term “heavy quark” — that its mass is sufficiently large compared to Λ so that $\alpha_s(m_Q)$, the effective coupling at the heavy quark mass, is in the perturbative region. This notion then refers to the charm, bottom and top quarks as heavy, *regardless of the magnitude of the typical energy scale (μ_{phy}) of the problem*. This view is taken in all next-to-leading order calculations on heavy quark production in the existing literature.[1, 25, 26]

As described earlier, the theoretical basis for a unified QCD treatment of heavy quark in the *relative* sense, suitable for all energy scales, already exists in the literature: it is based on the CWZ renormalization scheme which naturally implements the intuitive energy-scale-dependent *light* and *heavy* quark concepts.[8, 28] This scheme has been applied with good success to the calculation of Higgs boson via heavy quarks and gluons, effectively unifying the corresponding quark-scattering and gluon-fusion subprocesses in one consistent scheme which is valid at all energies.[29] This approach clearly also provides a natural framework for calculating the production of heavy quarks. It is particularly simple to implement in lepto-production processes, as already pointed out in a previous short communication.[30]

The present paper presents details of the method and the main physics results. For definiteness, we shall refer to this approach as the *variable (i.e., scale-dependent) flavor number scheme*, in contrast to the *fixed flavor number scheme* used in conventional calculations of heavy quark production.[25, 26] Since charged current and neutral current processes are treated in one uniform framework, we shall use the most general couplings for the vector gauge boson to the leptons and the quarks; and we shall keep the most general mass configurations for the quark lines in the hard cross-section calculation. The resulting complexity in kinematics, in the application of the factorization theorem of QCD, and in the calculation of hard matrix elements can be effectively handled using the helicity formalism. This aspect of the problem is formulated and presented in a separate paper,[31] hereafter referred to as I. Sec. 2 provides an overview of the scale-dependent parton flavor number scheme. Sec. 3 gives the detailed results on the order α_s gluon-fusion amplitudes. Sec. 4 discusses the subtraction procedure needed to make quark-scattering and gluon fusion mechanisms consistently co-exist. Sec. 5 presents the main physics results to show the relative impor-

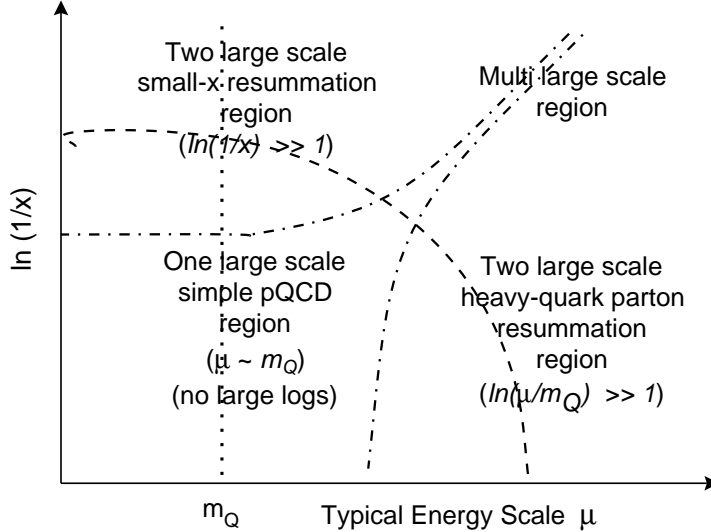


Figure 2: Regions of the $x - \mu_{phy}$ kinematic plane for a typical physical process involving a heavy quark with mass m_Q and the natural QCD calculational schemes for each region.

tance and interplay of the various contributions, as well as the reduced scale-dependence of the predictions. Finally, Sec. 6 recapitulates the theoretical issues and points to potential applications.

Since our approach effectively resums all large logarithms of the type $(\alpha_s \log \mu_{phy}/m_Q)^n$ which occur in fixed-parton-flavor-number calculations, it naturally extends the range of validity of the latter beyond the region $\mu_{phy} \sim O(m_Q)$. It does not, however, deal with the class of logarithms of the type $(\alpha_s \log s/\mu_{phy}^2)^n$ which is associated with the “small- x ” problem (typically, $x = \mu_{phy}/\sqrt{s}$). The latter has been the subject of several recent studies and it requires an entirely different method of resummation – the so-called k_t -factorization.[32, 33, 34] These two approaches are compatible and complementary: they both extend the region of applicability of the perturbative QCD calculations, but to different regions of phase space.³ This is illustrated schematically in a map of the $x - \mu$ kinematic plane, Fig. 2. Broadly speaking, our approach is needed when the typical energy scale μ_{phy} becomes large (compared to m_Q) for not-too-small x ; and the k_t -factorization method is necessary for very small- x and moderate μ_{phy} . What values of x must be considered as “small”, and μ_{phy}/m_Q as “large”, to require these improvements are open questions with no easy theoretical answers in perturbative QCD. (cf., the similar question: for what value of Q should Bjorken scaling set in?) However, these questions can be investigated phenomenologically by comparing numerical results from the different approaches in their regions of overlap. Existing numerical studies of the small- x resummation and conventional approaches suggest the latter maybe valid down to $x \sim 10^{-4}$.[35] The results presented later in this paper will shed some light on the comparison of scale-dependent and fixed parton flavor number schemes.

³A unified treatment is a topic for the future.

2 Overview of the Scheme and the Calculation

We consider a general lepton-hadron scattering process:

$$\ell_1(\ell_1) + N(P) \longrightarrow \ell_2(\ell_2) + Q(p_Q) + X(P_X), \quad (1)$$

to lowest order in the electro-weak interactions, as depicted in Fig. 3. In the final-state, we have required that there be a heavy quark Q of momentum p_Q^μ .⁴ We label the exchanged vector boson (γ , W , or Z) by B and its momentum by q .

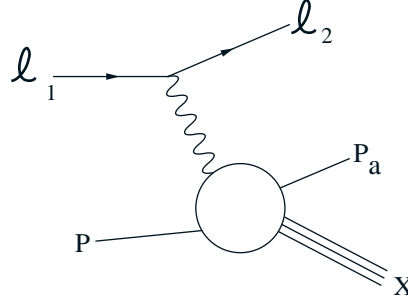


Figure 3: General lepton-hadron production amplitude for a heavy quark

2.1 Hadron Structure Functions and Factorization

After the calculable leptonic part of the cross section has been factored out, we work with the hadronic process induced by the virtual vector boson B :

$$B(q) + N(P) \longrightarrow Q(p_Q) + X(P_X), \quad (2)$$

and the cross-section is expressed in terms of the hadronic tensor

$$W^{\mu\nu} = \frac{1}{4\pi} \overline{\sum}_{X(P_X), \text{spin}} \langle P|J^\mu|P_Q, P_X\rangle (2\pi)^4 \delta^{(4)}(P + q - P_Q - P_X) \langle P_X, P_Q|J^{\nu\dagger}|P\rangle. \quad (3)$$

where $\overline{\sum}$ denotes a sum over all hadronic state q containing the final-state quark Q of momentum p_Q^μ .

The factorization theorem asserts that the hadronic tensor has the form^[6]

$$W_{BN}^{\mu\nu}(q, P, \dots) = f_N^a \otimes \hat{\omega}_{Ba}^{\mu\nu} = \sum_a \int \frac{d\xi}{\xi} f_N^a(\xi, \mu) \hat{\omega}_{Ba}^{\mu\nu}(q, k_a, \dots, \alpha_s(\mu)), \quad (4)$$

to the leading power of q^2 . Here $f_N^a(\xi, \mu)$ is the distribution function of parton a in the hadron N , and $\hat{\omega}_{Ba}^{\mu\nu}(q, k_a, \dots, \alpha_s(\mu))$ is the Wilson coefficient. That is, $\hat{\omega}_{Ba}^{\mu\nu}$ is the same kind of object as the hadronic tensor Eq. (3) except that it is evaluated on a parton target,

⁴We mean here a heavy quark in the absolute sense: $m_Q \gg \Lambda$, so that $\alpha_s(m_Q)$ is small enough to be in the perturbative regime. The heavy quark will be detected by its hadronization products.

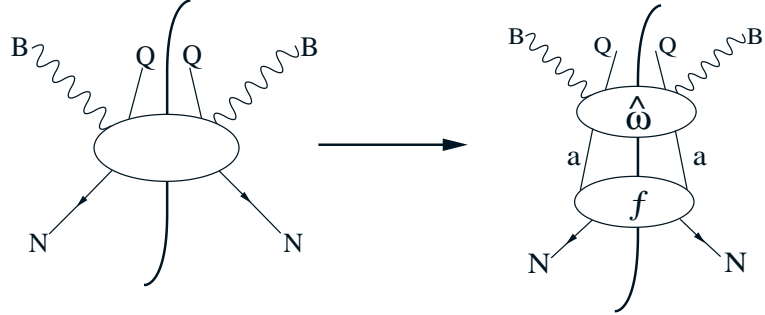


Figure 4: Graphical representation of the factorization formula, Eq. (5).

and that the long-distance contributions are subtracted off. The proof of the factorization theorem is to show that these long-distance pieces are all correctly taken account of by the factor of the parton density in Eq. (4).

The scale μ is the renormalization and factorization scale.⁵ Roughly speaking, μ sets the separation between the parts of the process that we attribute to long- and short-distance phenomena. The predictive power of the factorization theorem Eq. (4) arises when we set μ to a value of the order of a large physical scale in the problem, say $\mu \cdot b, q = \mu_{fac} = \mu_{ren} \approx \mu_{phy} \approx \sqrt{-q^2}$. Then the hard scattering (or Wilson) coefficient $\hat{\omega}$ may usefully be expanded in powers of the small coupling $\alpha_s(\mu)$. The μ dependence of the parton densities f_N^a is given by the Altarelli-Parisi equation, whose kernel is also perturbatively calculable in powers of $\alpha_s(\mu)$.

As explained in I^[31], in the presence of non-zero masses, it is the helicity amplitudes which provide the simplest connection between the physical (scalar) structure functions W_{BN} and the corresponding parton-level quantities $\hat{\omega}_{Ba}$. The factorization formula then reads:

$$W_{BN}^\lambda(Q^2, q \cdot p) = f_N^a \otimes \hat{\omega}_{Ba}^\lambda = \sum_a \int \frac{d\xi}{\xi} f_N^a(\xi, \mu) \hat{\omega}_{Ba}^\lambda \left(\frac{x}{\xi}, \frac{\hat{s}}{\mu}, \frac{m_Q}{\mu}, \alpha_s(\mu) \right), \quad (5)$$

where

$$W^\lambda = \epsilon_\mu^{(\lambda)*}(q, p) \cdot W^{\mu\nu} \cdot \epsilon_\nu^{(\lambda)}(q, p) \quad ; \quad \hat{\omega}^\lambda = \epsilon_\mu^{(\lambda)*}(q, k) \cdot \hat{\omega}^{\mu\nu} \cdot \epsilon_\nu^{(\lambda)}(q, k),$$

and $\epsilon_\nu^{(\lambda)}(q, r)$ is the polarization vector of the vector boson with momentum q and helicity λ ($= +, 0, -$) defined with respect to the reference vector r . (Since r is different in the definition of W^λ and $\hat{\omega}^\lambda$, the simple relation Eq. (5) is not an obvious consequence of Eq. (4); it follows only because the two reference momenta p and k are collinear, *cf.* I.) Fig. 4 depicts the factorization formula, Eq. (5), in a familiar form.

2.2 Masses and factorization schemes

The conventional method of calculation of the short-distance coefficients in this and other QCD processes is to set to zero the masses of internal lines and external partons in graphs for

⁵For simplicity, we do not distinguish between the factorization scale μ_{fac} and the renormalization scale μ_{ren} ; we set them equal to the same value μ .

the partonic subprocesses. Then the resulting infra-red poles (in dimensional regularization) are subtracted according the $\overline{\text{MS}}$ scheme. It can be shown that this implies that the ultra-violet divergences in the definitions of the parton densities are renormalized by the $\overline{\text{MS}}$ scheme also.

Setting quark masses to zero gives the leading term in an expansion of the short-distance coefficient in powers of m_Q/μ_{phy} . This is obviously inapplicable for a heavy quark if we want to treat the region where μ_{phy} is not much greater than m_Q . However, it is perfectly sensible to leave the heavy quark mass in the calculation of $\hat{\omega}$. We will later show how this works in a calculation, and we will verify that the $m_Q \rightarrow 0$ limit of the coefficient agrees with the standard zero mass calculation. The parton densities, including the one for the heavy quark, will continue to be defined by the $\overline{\text{MS}}$ scheme. In the case that the heavy quark is the charm quark, we will call this the “4-flavor scheme”.⁶

On the other hand, when $\mu_{phy} \ll m_Q$, one finds that there are large logarithms of the heavy quark mass in all perturbative calculations. That is, the 4-flavor scheme does not manifestly exhibit decoupling of the heavy quark. One obvious possibility is to use off-shell momentum-space subtractions (which exhibit explicit decoupling) instead of $\overline{\text{MS}}$. But this makes for much more complicated calculations, especially because of the complicated off-shell structure of the renormalization counterterms for gauge-invariant operators (such as are used to define the parton densities). The method of CWZ^[8] offers a natural and simple way: switch to a “3-flavor scheme” in this region.

Technically, the CWZ scheme is a hybrid of $\overline{\text{MS}}$ for the light partons and zero-momentum subtraction for graphs with a heavy quark line. The scheme has the following advantages: It satisfies manifest decoupling, and preserves gauge invariance. The evolution equations for the coupling and the parton densities are the same as for QCD with 3 flavors of quark and pure $\overline{\text{MS}}$ subtractions. Calculations are quite simple compared with the off-shell scheme. Finally, the charm quark density is zero to the leading power in Λ/m_c , so that the charm quark mass only appears in Wilson coefficients.

The 3-flavor scheme is appropriate when μ_{phy} is comparable to or less than about m_c . When other heavy quarks are present, one defines a series of schemes: 3-flavor, 4-flavor, 5-flavor etc. The N -flavor scheme is defined to treat the first N flavors of quark as light, and the remainder as heavy. It is appropriate when the physical scale of the process, μ_{phy} is above the mass of quark N and below that of quark $N + 1$. We will call N the number of *active* quarks.

The relation between schemes with different numbers of active flavors is just a case of a transformation between different renormalization and factorization schemes; and the matching conditions between the schemes have been calculated^[28, 37, 38]. At the one-loop level in the $\overline{\text{MS}}$ scheme, these are^[28] just that the coupling and parton densities are the same in the two schemes at $\mu = m_Q$. Thus a convenient way of implementing them is to use 3-flavor evolution below $\mu = m_c$, to use 4-flavor evolution above that point, with continuity at the break point. In this scheme, the use of $\mu = m_Q$ rather than, say, $\mu = 2m_Q$, is a matter of explicit calculation using $\overline{\text{MS}}$ subtraction, and is not a matter of arbitrary choice. There are higher order corrections to the matching conditions. Two-loop matching has been

⁶By keeping m_Q non-zero in the Wilson coefficient, the “theoretical inconsistency” described by Glück et al.^[36] does not occur in our approach. See further discussions in Sec. 4.1

calculated^[38] for the coupling, but not yet for the parton densities.

It is worth noting that existing NLO calculations of heavy quark production^[25, 26] essentially use the 3-flavor scheme as described above – for all energies, irrespective of the order of magnitude of μ_{phy} .

2.3 Contributing Partons and Parton Distributions

We use the term “variable flavor number scheme” to denote the scheme just described. It is implemented^[28] by using $\overline{\text{MS}}$ evolution with a number of active flavors that changes as one crosses the boundaries $\mu = m_Q$, where m_Q is the mass of a heavy quark (charm, bottom, etc.). The MT^[2] and CTEQ^[4] parton densities are defined using this method. Thus for a given scale μ for the parton densities, all quarks with mass less than μ are treated as partons (and thus have associated QCD-evolved parton distributions). For a quark Q with non-zero mass m_Q ($\gg \Lambda_{QCD}$), $f_N^Q(\xi, \mu)$ vanishes when $\mu \leq m_Q$ (*i.e.*, all the heavy quark dynamics in this region is in the Wilson coefficients). But when $\mu > m_Q$, $f_N^Q(\xi, \mu)$ satisfies the usual $\overline{\text{MS}}$ QCD evolution equation (with massless kernel functions) above threshold. Thus, there is no fixed restriction on the sum over parton flavor label a in the basic factorization formula Eq. (5): depending on the value of the relevant μ ($\sim \mu_{phy}$) of the physical process, the correct number of quark flavors appropriate for that energy scale will contribute.

This conceptual and calculational simplicity has an associated price. In the region just above the quark mass ($\mu \sim m_Q$), defining a parton distribution function for Q with massless evolution kernel appears to be somewhat artificial. Indeed the use of $f_N^Q(\xi, \mu)$ in a lowest order parton model formula for a cross section tends to overestimate the cross section, because the parton density does not contain the physical threshold behavior. The errors are compensated when one brings in higher order terms in the Wilson coefficient, as we will see. Although both schemes are equally correct, in principle, it would seem better to use a fixed parton flavor number around threshold, *e.g.*, 3 flavors for charm production. But as one goes higher in scale, one is genuinely in the overlap region, where the 3-flavor and 4-flavor schemes are equally valid. Eventually, the 4-flavor scheme becomes the one which describes the underlying physics more accurately.

2.4 Parton Structure Functions and Hard Scattering Mechanisms

In the variable flavor number scheme, for both charged current and neutral current production of heavy quarks, initial state quark-partons contribute through the vector-boson quark scattering (flavor excitation) subprocess, Fig. 1a and its higher-order corrections; whereas the gluon-parton contributes through the vector-boson gluon fusion (flavor creation) subprocess, Fig. 1b, and its higher-order corrections. The order α_s^0 quark scattering hard amplitude $\omega_{BQ}^{\lambda(0)}$ is easy to calculate. Since it is obtained from a simple tree diagram, we can identify it with the corresponding hard amplitude $\hat{\omega}_{BQ}^{\lambda(0)}$ which enters the factorization formula, Eq. (4). In our framework, the explicit results are given in I (Sec. 5 and Appendix C). The order α_s^1 parton level gluon fusion amplitudes $\omega_{Bg}^{\lambda(1)}$ are also relatively straightforward to evaluate since they are free from singularities when all the quark masses

are kept finite.⁷

Note the distinction between the notations $\hat{\omega}$ and ω for the structure functions for the partonic subprocesses. *The unadorned ω will be a partonic structure function⁸ without subtractions, but with non-zero quark masses.* In the zero mass limit ω will be divergent. The hatted quantity $\hat{\omega}$ will have subtractions to remove the infra-red dependence. It is the subtracted partonic structure function $\hat{\omega}$ that is to be used in the factorization theorem Eq. (4).

We will present the detailed formulas for ω and $\hat{\omega}$, in the helicity formalism we use, later in Sec. 3. Here we focus on the relation between the unsubtracted ω and the subtracted $\hat{\omega}$ at order α_s in order to elucidate the underlying principles. As is well known, this relationship is established by applying the factorization formula at the parton amplitude level. This provides the exact relation, to this order:

$$\begin{aligned}\omega_{Bg}^{\lambda(1)} &= \sum_a f_g^a \otimes \hat{\omega}_{Ba}^{\lambda} = \sum_a (f_g^{a(0)} \otimes \hat{\omega}_{Ba}^{\lambda(1)} + f_g^{a(1)} \otimes \hat{\omega}_{Ba}^{\lambda(0)}) \\ &= \hat{\omega}_{Bg}^{\lambda(1)} + f_g^{Q(1)} \otimes \omega_{BQ}^{\lambda(0)},\end{aligned}\quad (6)$$

where we made use of the fact that $f_b^{a(0)}(\xi) = \delta_b^a \delta(1 - \xi)$, $\hat{\omega}_{Ba}^{\lambda(0)} = \omega_{Ba}^{\lambda(0)}$, and Bg scattering begins at order 1. The order α_s quark distribution inside an on-shell gluon, $f_g^{Q(1)}$, is given by

$$f_g^{Q(1)} = \frac{\alpha_s(\mu)}{2\pi} \ln \frac{\mu^2}{m_Q^2} P_{gQ}, \quad (7)$$

where we have used the $\overline{\text{MS}}$ prescription to renormalize the ultra-violet divergences in the quark density. Since we have kept a non-zero quark mass, there is no infra-red divergence. In this formula, P_{gQ} is the familiar $g \rightarrow Q\bar{Q}$ splitting function $P_{gQ}(\xi) = \frac{1}{2}(1 - 2\xi + 2\xi^2)$. Eq. (7) follows from the Feynman rules for parton densities, and it is quite accidental that there is no constant term, but only the logarithm times the splitting function. By inverting Eq. (6), we obtain the formula for the requisite hard amplitude:

$$\hat{\omega}_{Bg}^{\lambda(1)} = \omega_{Bg}^{\lambda(1)} - f_g^{Q(1)} \otimes \omega_{BQ}^{\lambda(0)}. \quad (8)$$

The second term on the right-hand side (henceforth referred to as the *subtraction term*), represents that part of the gluon fusion term which at large μ_{phy}^2 has the internal quark line relatively close to the mass-shell and almost collinear to the gluon.

2.5 Complete NLO (order α_s) Hadron Structure Functions

Combining these results, we obtain the formula for the physical helicity structure functions for heavy quark production on a hadron target:

$$W_{BN}^{\lambda} = f_N^Q \otimes \omega_{BQ}^{\lambda(0)} - \sum_i f_N^g \otimes f_g^{Q_i(0)} \otimes \omega_{BQ_i}^{\lambda(0)} + f_N^g \otimes \omega_{Bg}^{\lambda(1)} + O(\alpha_s^2). \quad (9)$$

⁷In the conventional calculation of photo- and lepto-production of heavy quarks in the fixed parton flavor number scheme^[25, 26] these are sometimes called Born terms because they represent the leading order contribution to the flavor creation mechanisms. Since the flavor excitation mechanism actually come in with one less power of α_s , we shall state the explicit powers of α_s to avoid confusion.

⁸We make a clear distinction between the concepts of ‘structure function’ and ‘parton density’, contrary to common usage.

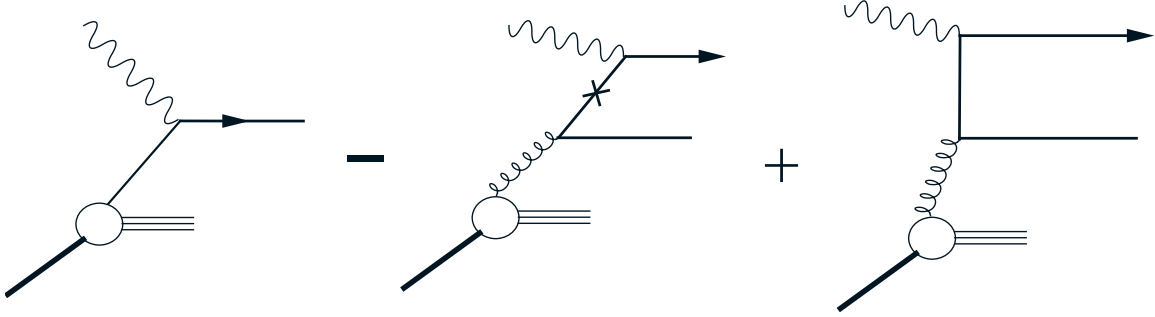


Figure 5: Graphical representation of the three terms which enter the *master equation*, Eq. (9), for the physical structure functions: the subtraction term is placed in the middle to emphasize its similarity both to the quark-scattering (left) and to the gluon-fusion (right) contributions. The \times on the internal quark line in the subtraction term indicates it is close to mass-shell and collinear to the gluon and the hadron momenta.

Note that, in the case of a neutral current process, a sum over the two heavy quarks (quark and antiquark) in the final state is needed. This is the basic QCD equation for lepto-production of heavy quark production in our approach. The subtraction term is placed in the middle to emphasize its similarity both to the quark-scattering (left) and to the gluon-fusion (right) contributions. On one hand, this term overlaps with the first (quark scattering) one due to the common factor $\omega_{BQ}^{\lambda(0)}$ and the approximate equality

$$f_N^Q(\xi, \mu) \simeq f_g^{Q(1)} \otimes f_N^g \quad \text{when } \mu > m_Q \text{ and } \alpha_s \log \frac{\mu}{m_Q} \sim O(1), \quad (10)$$

where $f_g^{Q(1)}$ is given by Eq. (7).⁹ On the other hand, its close connection to the last (gluon fusion) term originates from Eq. (8). Since it represents the part of the gluon-fusion term which is already included in a fully QCD-evolved quark-scattering term, a consistent formalism must lead to its subtraction to avoid double counting, as naturally happens here. Fig. 5 illustrates the same point graphically. (For clarity, we only show one-half of the cut-diagrams for this process, *cf.*, Fig. 4.) The \times on the internal quark line in the subtraction term denotes the following operation: In the hard scattering part of the middle graph, that is, the upper part of the graph, the incoming quark's momentum is replaced by an on-shell value with zero transverse momentum. This replacement gives a good approximation when the quark is collinear to the gluon, and results in a factor of the order α_s distribution of a quark in a gluon, Eq. (7).

The physics behind this formula should be well-known to students of the conventional QCD parton model for light quarks.¹⁰ However, this formalism has not been invoked in existing calculations of heavy quark production.^[1, 25, 26] Rather, they typically use the scheme in which the heavy quark only appears in the Wilson coefficients (*e.g.*, a 3-flavor

⁹It is straightforward to demonstrate that this expression satisfies the leading order QCD evolution equation with the correct boundary condition $f_N^Q(\xi, \mu = m_Q) = 0$.

¹⁰Although the nature of the subtraction term is usually not transparent to most non-experts since, for zero-mass quarks, it is usually identified only as the coefficient of a $1/\epsilon$ pole in the most commonly used $\overline{\text{MS}}$ calculational scheme.

scheme for charm production and a 4-flavor scheme for bottom production). In that case, the quark-scattering (flavor-excitation) contribution is excluded whenever $m_Q \neq 0$, no subtraction from the gluon-fusion contribution is applied in those calculations. There are calculations that allow the heavy quark to have a parton density, and thus work well above the quark threshold. But these normally set the quark mass to zero in the Wilson coefficients and thus are not good approximations when the process is not sufficiently far above the quark threshold. (*Cf.* Ref. [36].)

The variable parton-flavor-number scheme for calculating heavy quark production thus represents a natural and correct extension of the usual zero-quark-mass QCD parton framework to the case of non-zero quark mass. (We avoid using the word “heavy”, at least temporarily, since at this point “light” and “heavy” are relative with respect to the typical energy scale in this approach.) This scheme contains all the ingredients of a consistent QCD theory of heavy quark production over a wide range of energy scales as mentioned in Sec. 1. In particular, if the initial-state quark (labeled by Q in Eq. (9)) is massive and the typical energy scale μ_{phy} is of the same order as m_Q , then Eq. (10) implies an approximate cancellation of the first two terms on the right-hand side of Eq. (9) — thus we arrive at $W_{BN}^\lambda \simeq f_N^g \otimes \omega_{Bq}^{\lambda(1)}$ — *i.e.*, dominance of the gluon-fusion mechanism — which reproduces the usual picture of heavy quark production in the fixed parton flavor number scheme. (This is the region labeled “one large scale ($m_Q \sim \mu_{phy}$)” in Fig. 2.)

On the other hand, if either Q is a usual light quark (*i.e.*, $m_Q \approx 0$) or Q is massive but $\mu_{phy} \gg m_Q$, Eq. (10) does not hold; instead, the subtraction term becomes the dominant piece of the gluon fusion contribution (because it has the large logarithmic factor $\frac{\alpha_s(\mu)}{2\pi} \ln \frac{\mu^2}{m_Q^2}$ embodying a “collinear divergence”), hence the last two terms almost cancel (leaving only a *correction term* of order $\frac{\alpha_s(\mu)}{2\pi}$ with no large logarithm factor) and we obtain $W_{BN}^\lambda = f_N^Q \otimes \omega_{BQ}^{\lambda(0)} + O(\alpha_s)$ — which reproduces the leading order QCD parton model picture appropriate for energies much higher than all masses. (This is the region labeled “two large scales ($1 \gg m_Q/\mu_{phy}$)” in Fig. 2.)

Eq. (9) provides a smooth interpolation between the two kinematic regions described above, and contains both as special cases. Because the subtraction term represents precisely the overlap of the other two, a change in the factorization scale amounts explicitly to a reshuffling between the three terms on the right hand side of Eq. (9). The differences arising from a change in the factorization scale are genuinely of higher order in α_s , hence are smaller by a factor α_s than if one or more terms are left out.¹¹ We will demonstrate this point in detail in Sec. 5. The differences can be made smaller by using higher order terms in perturbation theory.

Strictly speaking, Eq. (9) is incomplete: we should also add order α_s quark-scattering contributions of the form $f_N^Q \otimes \omega_{BQ}^{\lambda(1)} - f_N^Q \otimes f_Q^{Q'(1)} \otimes \omega_{BQ'}^{\lambda(0)}$. The ideas are exactly the same as discussed above for the order α_s gluon contributions; but these terms are numerically less important because we have many more gluons inside the hadron than sea quarks. (In this sense, the order α_s Bq scattering terms are *effectively one order higher* since, for sea quarks, $f_N^Q \sim f_N^g \otimes f_g^{Q'(1)}$ is of order α_s compared to the gluon distribution f_N^g .) We should also mention that Eq. (9) can be generalized to higher orders by the systematic application of

¹¹But remember that the gluon distribution is often much larger numerically than a quark distribution.

the above scheme. The order α_s^2 hard amplitudes will be given by formulas generalized from Eq. (8). The differences between these and the corresponding ones already calculated in the conventional fixed-number-of-flavor scheme are finite pieces attributable to the change of renormalization scheme.

3 One-loop Gluon-Initiated Parton Structure Functions

The one-loop forward hard amplitudes for the $2 \rightarrow 2$ vector-boson-gluon scattering process

$$B(q) + g(k) \rightarrow \bar{q}_1(p_1) + q_2(p_2) \quad (11)$$

are given by the cut diagrams shown in Fig. 6. As indicated, we use q to denote the momentum of the vector boson, k the momentum of the gluon in the initial state, and (p_1, p_2) the momenta of the quarks in the final state. For flavor changing charged current processes (vector boson $B = W^\pm$), the subscript 1(2) will be associated with the light (heavy) quark; for neutral current processes ($B = \gamma, Z$), both are associated with the heavy quark.

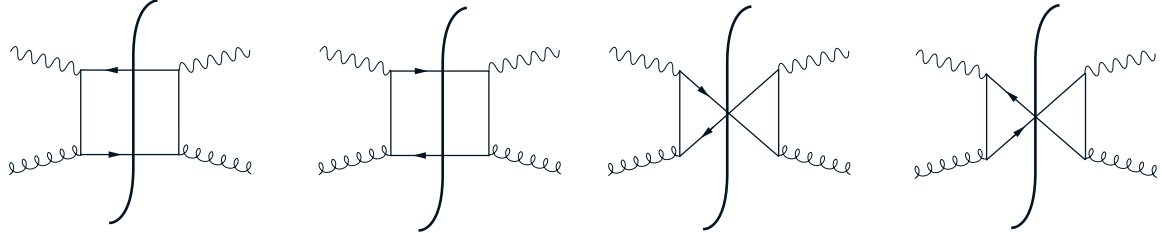


Figure 6: Cut diagrams for order α_s^1 vector-boson gluon scattering.

Since we keep the masses of the quarks (m_1, m_2) non-zero, these diagrams do not contain any singularities: they are infra-red finite since the gluon only appears in the initial state; and the internal virtual quark lines never go on mass-shell due to the finite masses. Thus it is safe to perform the calculation in 4-dimensional space-time. The parton tensor (cut) amplitudes are represented by:

$$\omega^{\mu\nu}(q, k, p_1) = \frac{1}{4\pi} \sum_i \int d\Gamma_2 \frac{N_i^{\mu\nu}}{P_1^i P_2^i}, \quad (12)$$

where i labels the diagrams; $d\Gamma_2$ is the two-particle final-state phase space differential; and $P_1^i P_2^i$ denotes the two propagator factors appropriate for diagram i .

As mentioned earlier, we find it most convenient to work with helicity structure functions. They are:

$$\begin{aligned} \omega^\lambda(Q^2, \hat{s}, m_1^2, m_2^2) &= \frac{1}{4\pi} \sum_i \int d\Gamma_2 \frac{N_i^\lambda}{P_1^i P_2^i} \\ N_i^\lambda &= \epsilon_\mu^{(\lambda)*}(q, k) \cdot N_i^{\mu\nu} \cdot \epsilon_\nu^{(\lambda)}(q, k), \end{aligned} \quad (13)$$

where $\epsilon_\nu^{(\lambda)}(q, k)$ is the polarization vector of the vector boson with helicity λ ($= +, 0, -$) defined with respect to k . For the general case, the helicity amplitudes exhibit a natural

symmetry if we express the vector-boson-quark vertex in terms of the two chiral coupling constants: $g_{R,L}$. The amplitudes ω^λ (and N_i^λ) are quadratic in the g' s, and we can write

$$\omega^\lambda = \frac{\alpha_s(\mu)}{\pi} \sum_{\kappa} C_\kappa \cdot \omega_\kappa^\lambda \quad (\kappa = s, x, a) \quad (14)$$

with the chiral coupling combinations (symmetric, anti-symmetric, and crossed):

$$C_{s,a} = g_R^2 \pm g_L^2 \quad ; \quad C_x = 2g_R g_L.$$

It is convenient to express the results in terms of center-of-mass variables of the parton process. We have

$$\begin{aligned} k^\mu &= (k, 0, 0, k) \\ q^\mu &= (E_q, 0, 0, -k) \\ p_1^\mu &= (E_1, p \sin \theta, 0, p \cos \theta) \\ p_2^\mu &= (E_2, -p \sin \theta, 0, -p \cos \theta) \end{aligned} \quad (15)$$

where the initial state energy and momenta are

$$\begin{aligned} k &= (\hat{s} + Q^2)/(2\sqrt{\hat{s}}) \\ E_q &= (\hat{s} - Q^2)/(2\sqrt{\hat{s}}) \end{aligned}$$

and the final state variables are

$$\begin{aligned} p &= \Delta(\hat{s}, m_2^2, m_1^2)/(2\sqrt{\hat{s}}) \\ E_1 &= (\hat{s} - m_2^2 + m_1^2)/(2\sqrt{\hat{s}}) \\ E_2 &= (\hat{s} + m_2^2 - m_1^2)/(2\sqrt{\hat{s}}) \end{aligned} \quad (16)$$

with $\Delta(a, b, c) \equiv \sqrt{a^2 + b^2 + c^2 - 2ab - 2bc - 2ca}$.

There are two types of logarithmic terms arising from the phase space integration of the propagator factors in the t and u channels, respectively:

$$\begin{aligned} L_t &= \log \left(\frac{E_1 + p}{E_1 - p} \right) \equiv \log \left[\frac{(\hat{s} - m_2^2 + m_1^2 + \Delta(\hat{s}, m_2^2, m_1^2))^2}{4m_1^2 \hat{s}} \right], \\ L_u &= \log \left(\frac{E_2 + p}{E_2 - p} \right) \equiv \log \left[\frac{(\hat{s} + m_2^2 - m_1^2 + \Delta(\hat{s}, m_2^2, m_1^2))^2}{4m_2^2 \hat{s}} \right]. \end{aligned} \quad (17)$$

3.1 General mass case (Flavor changing charge current interaction)

For general masses $\{m_1, m_2\}$, the independent right-handed helicity structure functions are:

$$\begin{aligned} \omega_s^+ &= L_t \left[\frac{1}{2} + \frac{E_1}{k} \left(\frac{E_1}{k} - 1 \right) \right] - \frac{2p}{\sqrt{\hat{s}}} \left(\frac{E_q}{k} \right)^2 \\ &+ L_u \left[\frac{1}{2} + \frac{E_2}{k} \left(\frac{E_2}{k} - 1 \right) \right] \\ \omega_x^+ &= (L_t + L_u) \frac{2m_1 m_2}{(Q^2 + \hat{s})^2} (\hat{s} - (m_2^2 + m_1^2)) - \frac{8m_1 m_2 p \sqrt{\hat{s}}}{(Q^2 + \hat{s})^2} \\ \omega_a^+ &= L_t \left[\frac{1}{2} + \frac{E_1}{k} \left(\frac{E_1}{k} - 1 \right) + \frac{m_1^2(m_2^2 - m_1^2)}{2\hat{s}k^2} \right] + \frac{p(m_2^2 - m_1^2)}{k^2 \sqrt{\hat{s}}} \\ &- L_u \left[\frac{1}{2} + \frac{E_2}{k} \left(\frac{E_2}{k} - 1 \right) + \frac{m_2^2(m_1^2 - m_2^2)}{2\hat{s}k^2} \right], \end{aligned} \quad (18)$$

where the subscripts (s, x, a) refer to the chiral combinations of Eq. (14).

The longitudinal helicity ones are:

$$\begin{aligned}
\omega_s^0 &= -(L_t + L_u) \left[\frac{(m_2^2 + m_1^2)(Q^4 - (m_2^2 - m_1^2)^2 - 2\hat{s}k^2)}{4\hat{s}Q^2k^2} \right. \\
&\quad \left. - \frac{E_q}{2k^2\sqrt{\hat{s}}} \left(m_2^2 + m_1^2 - \frac{(m_2^2 - m_1^2)^2}{Q^2} \right) + \frac{m_2^2m_1^2}{k^2\hat{s}} \right] \\
&\quad - (L_t - L_u) \frac{E_q(m_2^2 - m_1^2)}{k^2\sqrt{\hat{s}}} \\
&\quad + \frac{p}{k^2Q^2\sqrt{\hat{s}}} [(m_2^2 - m_1^2)^2 + Q^2(2Q^2 - (m_2^2 + m_1^2))] \\
\omega_x^0 &= -(L_t + L_u) m_1 m_2 \left[\frac{1}{Q^2} + \frac{\hat{s} - (m_2^2 + m_1^2)}{2k^2\hat{s}} \right] + \frac{2m_1 m_2 p}{k^2\sqrt{\hat{s}}} \\
\omega_a^0 &= 0.
\end{aligned} \tag{19}$$

And the left-handed helicity structure functions ω_κ^- are related to the right-handed ones by the symmetry relations:

$$\omega_s^- = \omega_s^+, \quad \omega_x^- = \omega_x^+, \quad \omega_a^- = -\omega_a^+. \tag{20}$$

3.2 Equal mass case (Flavor non-changing neutral current interaction)

When the masses are equal, $m_1 = m_2 = m$, we obtain, as a special case of the above:

$$\begin{aligned}
L_t = L_u = L &= 2 \log \left[\frac{\sqrt{\hat{s}} + \sqrt{\hat{s} - 4m^2}}{2m} \right] \\
\omega_a^0 &= \omega_a^- = \omega_a^+ = 0
\end{aligned}$$

and

$$\begin{aligned}
\omega_s^+ = \omega_s^- &= L \frac{(Q^4 + \hat{s}^2)}{(Q^2 + \hat{s})^2} - \frac{(\hat{s} - Q^2)^2 \Delta}{\hat{s}(Q^2 + \hat{s})^2} \\
\omega_x^+ = \omega_x^- &= L \frac{4m^2(\hat{s} - 2m^2)}{(Q^2 + \hat{s})^2} - \frac{4m^2 \Delta}{(Q^2 + \hat{s})^2} \\
\omega_s^0 &= -L \frac{2m^2(4m^2Q^2 + 3Q^4 - 4Q^2\hat{s} - \hat{s}^2)}{Q^2(Q^2 + \hat{s})^2} + \frac{4(Q^2 - m^2)\Delta}{(Q^2 + \hat{s})^2} \\
\omega_x^0 &= -L \frac{2m^2(-4m^2Q^2 + Q^4 + 4Q^2\hat{s} + \hat{s}^2)}{Q^2(Q^2 + \hat{s})^2} + \frac{4m^2 \Delta}{(Q^2 + \hat{s})^2}
\end{aligned} \tag{21}$$

where

$$\Delta \equiv \Delta(\hat{s}, m^2, m^2) = \sqrt{\hat{s}(\hat{s} - 4m^2)}.$$

4 Mass-singularities, Collinear Divergences, Subtractions and Infrared-safe Amplitudes

In the fixed parton-flavor-number calculational scheme, the results of the last section represent the full answer to the vector-boson-gluon fusion production of heavy quarks at the

order α_s level. These results contain terms which become large as one (or both) of the quark masses are small compared to the characteristic energy scale. These *mass singularity terms* are isolated by taking the m_1 (m_2) $\rightarrow 0$ limits of Eq. (18-20). They arise from the configuration in the phase space integration when an internal quark line becomes almost on-shell¹² and collinear to the initial state gluon. In our scheme with scale-dependent parton-flavor-number, these terms are included in the quark scattering contribution with properly evolved quark parton distributions. As explained in Sec. 2.5 the QCD formalism provides a natural procedure to subtract these terms from the gluon-fusion amplitudes to avoid double counting. In this section, we identify the subtraction terms in some detail.

4.1 Unequal Mass (flavor-changing) Case ($m_1 \rightarrow 0$)

In the limit $m_1 \rightarrow 0$, we drop all m_1 dependencies in Eq. (18-20) except inside the logarithm where the mass singularity resides. We also replace m_2 by m_Q to emphasize that the remaining mass is associated with a quark that is heavy in absolute terms (*i.e.*, compared to Λ). The arguments of the t - and u -channel logarithmic factors become

$$\begin{aligned} L_t &= \log \frac{E_1 + p}{E_1 - p} = \log \frac{(E_1 + p)^2}{m_1^2} \rightarrow \log \frac{4p^2}{m_1^2} \\ L_u : \quad \log \frac{E_2 + p}{E_2 - p} &= \log \frac{(E_2 + p)^2}{m_2^2} \rightarrow \log \frac{\hat{s}}{m_Q^2} \end{aligned} \quad (22)$$

where the magnitude of the quark 3-momenta is given by $p^2 = (\hat{s} - m_Q^2)^2/(2\hat{s})$. We note that L_t is the only factor which contains the *mass singularity* associated with $m_1 \rightarrow 0$. It arises from the collinear integration region of the t -channel propagator factor over the quark transverse momentum, Fig. 6a,b,c. This is seen as follows: in the limit under consideration, the singular factor in the integrand of Eq. (13) is $1/(t - m_1^2) \propto 1/(p_t^2 + m_1^2)$. We can take the $m_1 \rightarrow 0$ limit everywhere except in this factor where it must be retained to cut off the collinear (*i.e.* $p_t = 0$) singularity. The leading behavior is obtained by keeping the constant term of the Taylor expansion of the numerator function in p_t^2 . We obtain therefore,

$$\int_0^{p_{t \max}^2} \frac{dp_t^2}{p_t^2 + m_1^2} = \log \frac{p_{t \max}^2}{m_1^2} = L_t + O(1) \quad (23)$$

where we used $p = p_{t \max}$ for the quark lines, and explicitly displayed the role of m_1^2 as the cutoff for the collinear singularity.

Isolation of Infrared-sensitive terms:

We can isolate the mass (collinear) singularity from the (process-dependent) dynamics by writing

$$L_t = \log \frac{\mu_f^2}{m_1^2} + \log \frac{4p_{t \max}^2}{\mu_f^2} \quad (24)$$

where we have introduced an arbitrary scale parameter μ_f — the factorization scale — which separates the low p_t *collinear* region from the true *hard scattering* region. For an appropriately chosen μ_f (*e.g.*, some external physical scale *independent of* \hat{s}), the first term

¹²Relative to Q^2 .

on the right-hand side (the collinear term) contains the mass singularity which is to be subtracted from the gluon-fusion contribution (to make it infra-red safe) and resummed into the QCD evolved quark distribution function in the quark-scattering contribution.

The infra-red sensitive terms can be collected by substituting Eq. (24) in Eq. (18-20). We obtain the following non-vanishing amplitudes:

$$\begin{aligned}\omega_s^{IR+} &= 1 \cdot P_{g \rightarrow q}(\tilde{x}_m) \log \left(\frac{\mu_f^2}{m_1^2} \right) \\ \omega_a^{IR+} &= 1 \cdot P_{g \rightarrow q}(\tilde{x}_m) \log \left(\frac{\mu_f^2}{m_1^2} \right) \\ \omega_s^{IR0} &= \frac{m_Q^2}{Q^2} \cdot P_{g \rightarrow q}(\tilde{x}_m) \log \left(\frac{\mu_f^2}{m_1^2} \right)\end{aligned}\quad (25)$$

with \tilde{x}_m denoting the scaling variable,

$$\tilde{x}_m = \tilde{x} \left(1 + \frac{m_Q^2}{Q^2} \right) ; \quad \tilde{x} = \frac{Q^2}{2k \cdot q} = \frac{Q^2}{\hat{s} + Q^2} \quad (26)$$

and $P_{g \rightarrow q}$ the usual gluon to quark splitting function,

$$P_{g \rightarrow q}(x) = \frac{1}{2}[(1-x)^2 + x^2] \quad (27)$$

They are exactly proportional to the leading order quark scattering amplitudes in the same limit. Comparing Eq. (25) with the order α_s^0 result from paper I, we obtain:

$$\omega_{Bg}^{IR\lambda} = \omega_{Bq}^{\lambda(0)}(m_1 = 0) \cdot \frac{\alpha_s}{2\pi} P_{g \rightarrow q}(\tilde{x}_m) \theta(\mu_f - m_1) \log \frac{\mu_f^2}{m_1^2} \quad (\text{for all } \lambda) \quad (28)$$

This is anticipated in the discussion of the factorization theorem in Sec. 2, *cf.* the second term on the right-hand side of Eq. (6).

Mass (Collinear) Subtraction and Infrared-safe Amplitudes:

As explained in Sec. 2, the collinear configuration from which the above infrared sensitive amplitudes originate corresponds physically to the overlapping region of the quark scattering and gluon fusion production mechanisms. We need to subtract these amplitudes from ω_{Bg}^λ to avoid double counting and to obtain *infra-red safe hard gluon scattering amplitudes* $\hat{\omega}_{Bg}^\lambda$ (*cf.* Eq. (8)). We have a certain freedom in choosing the subtraction terms: as long as they contain the leading infrared sensitive terms identified above, any specific choice made for these overlapping terms effectively defines the factorization scheme inherent in the master (factorization) equation, Eq. (9). However, this freedom must be constrained by two consistency requirements. On the one hand, the order α_s^0 quark amplitude $\omega_{Bq}^{\lambda(0)}$ should be identical in its two occurrences in Eq. (9). On the other hand, the logarithmic term in Eq. (28) must agree with the scheme used to define parton densities.

There is a certain amount of choice possible.

We consider the case of unequal masses, one large and one small: $m_2 \approx \mu_f = \mu_{phy} \gg m_1 \gg \Lambda_{QCD}$. Then the parton density that is needed for quark 1 is defined by \overline{MS} . Consider

$\omega_{Bq_1}^{\lambda(0)}$, which is given by the Born graph for scattering off the relatively light quark 1 to make the heavy quark 2. There are two obvious choices for the value of m_1 in $\omega_{Bq}^{\lambda(0)}$: either replace the mass m_1 of the lighter quark to zero, or leave it at the physical value. When m_1 is small compared with the physical scale for the hard scattering, μ_{phy} , it certainly does not matter what we do, since Wilson coefficients have a finite zero-mass limit. But our formalism also extends to the region where m_1 is not negligible. Then the physics is correctly given by the order α_s graph for Bg fusion, the third term $\omega_{Bq}^{\lambda(1)}$ in Eq. (9) — with the mass m_1 kept at its physical value. (This is the region where the 3-flavor scheme applies and it treats m_1 as “heavy”.) For consistency, it is then advantageous to keep m_1 also non-zero in the order α_s^0 Wilson coefficient $\omega_{Bq}^{\lambda(0)}$ even if this is not absolutely required by the formalism — the first two terms in the master equation are guaranteed to cancel near threshold (*cf.* Sec. 2.5) as long as the same choice of $\omega_{Bq}^{\lambda(0)}$ is made in both terms.

Thus we shall define the subtraction term as

$$\omega_{Bq}^{Sub\ \lambda} = \omega_{Bq}^{\lambda(0)}(Q^2, m_1, m_Q) \cdot \frac{\alpha_s}{2\pi} P_{g \rightarrow q}(\tilde{x}_m) \theta(\mu_f - m_1) \log \frac{\mu_f^2}{m_1^2} \quad (\text{for all } \lambda). \quad (29)$$

with the full mass dependencies in $\omega_{Bq}^{\lambda(0)}(\hat{s}, m_1, m_Q)$, and with the understanding that the same choice of $\omega_{Bq}^{\lambda(0)}$ is to be made in the order α_s^0 quark-scattering term in the master equation, Eq. (9). The choice of the $\overline{\text{MS}}$ scheme for the parton densities implies the precise formula given in Eq. (29), which has a logarithmic term, but no constant term. This follows from a calculation of the one-loop density of a massive quark in an on-shell gluon.

The properly subtracted, *infra-red safe hard gluon scattering amplitudes* are then given by

$$\hat{\omega}_{Bq}^{\lambda}(\hat{s}, Q^2, m_1, m_Q, \mu_f) = \omega_{Bq}^{\lambda}(\hat{s}, Q^2, m_1, m_Q) - \omega_{Bq}^{Sub\ \lambda}(Q^2, m_1, m_Q, \mu_f) \quad (30)$$

with $\omega_{Bq}^{\lambda}(\hat{s}, Q^2, m_1, m_Q)$ given by Eqs. (18)-(20) of Sec. 3.1 and $\omega_{Bq}^{Sub\ \lambda}(Q^2, m_1, m_Q, \mu_f)$ by Eq. (29) above respectively.

The explicit expressions for $\hat{\omega}_{Bq}^{\lambda}$ in the general case is not particularly illuminating. We give below the results in the $m_1 \rightarrow 0$ limit:

$$\begin{aligned} \hat{\omega}_s^+ &= P_{g \rightarrow q}(\tilde{x}_m) \log \frac{4p_{t\max}^2}{\mu_f^2} - \frac{\tilde{x}(1-2\tilde{x})^2}{(1-\tilde{x})} \frac{(s-m_Q^2)}{Q^2} \\ &\quad + L_u \left[P_{g \rightarrow q}(\tilde{x}_m) + 2\tilde{x}(1-2\tilde{x}) \frac{m_Q^2}{Q^2} \right] \\ \hat{\omega}_a^+ &= P_{g \rightarrow q}(\tilde{x}_m) \log \frac{4p_{t\max}^2}{\mu_f^2} + (2\tilde{x}^2) \frac{m_Q^2(s-m_Q^2)}{Q^4} \\ &\quad - L_u \left[P_{g \rightarrow q}(\tilde{x}_m) + 2\tilde{x}(1-2\tilde{x}) \frac{m_Q^2}{Q^2} - 2\tilde{x}^2 \left(\frac{m_Q^2}{Q^2} \right)^2 \right] \\ \hat{\omega}_x^+ &= 0 \\ \hat{\omega}_s^0 &= \frac{m_Q^2}{Q^2} P_{g \rightarrow q}(\tilde{x}_m) \log \frac{4p_{t\max}^2}{\mu_f^2} + (2\tilde{x}^2) \frac{(m_Q^4 - m_Q^2 Q^2 + 2Q^4)(s-m_Q^2)}{Q^6} \\ &\quad + L_u \frac{m_Q^2}{Q^2} \left[\frac{1+6\tilde{x}-14\tilde{x}^2}{2} - \tilde{x}(1-2\tilde{x}) \frac{m_Q^2}{Q^2} + \tilde{x}^2 \left(\frac{m_Q^2}{Q^2} \right)^2 \right] \\ \hat{\omega}_x^0 &= \hat{\omega}_a^0 = 0 \end{aligned} \quad (31)$$

Of course, for energy scales much larger then m_2 (m_Q), there is also a mass singularity associated with the factor $\log(m_2/\mu_f)$ which resides in L_u . In our approach, an infra-red sensitive term analogous to Eq. (28) with $m_1 \leftrightarrow m_2$ should then be subtracted from the order α_s gluon-fusion amplitudes. The subtracted part, again, is included in the corresponding order α_s^0 quark scattering amplitude — with incoming quark “2” — which represents the resummed result of all such terms to arbitrary orders. The resummation is performed by the Altarelli-Parisi evolution of the parton densities.

4.2 Equal Mass Case ($m_1 = m_2 = m \rightarrow 0$) and Comparison with \overline{MS} scheme results

Corresponding results for the case of flavor non-changing neutral current interactions can be obtained from the above general results by setting $m_1 = m_2 = m$ and choosing the appropriate couplings. We give a few explicit formulas for illustrative purpose and for establishing the relation of our subtraction scheme to the \overline{MS} scheme. For the equal mass case, the infra-red sensitive logarithm factor is

$$L = \log \frac{4p_{t \max}^2}{m^2} = \log \frac{\hat{s}}{m^2} = \log \frac{\mu_f^2}{m^2} + \log \frac{\hat{s}}{\mu_f^2}$$

In the $m \rightarrow 0$ limit, the non-vanishing helicity amplitudes are (keeping m only in the other-wise divergent logarithm)

$$\begin{aligned} \omega_s^+ &= \omega_s^- = 2P_{g \rightarrow q}(\tilde{x}) \log \frac{\hat{s}}{m^2} - (1 - 2\tilde{x})^2 \\ \omega_s^0 &= 4(1 - \tilde{x})\tilde{x} \end{aligned} \quad (32)$$

After subtracting the mass-singularity, we obtain the infra-red safe hard amplitudes for zero mass quarks

$$\begin{aligned} \hat{\omega}_s^+ &= \hat{\omega}_s^- = 2P_{g \rightarrow q}(\tilde{x}) \log \frac{\hat{s}}{\mu_f^2} - (1 - 2\tilde{x})^2 \\ &= 2P_{g \rightarrow q}(\tilde{x}) \left(\log \frac{Q^2}{\mu_f^2} + \log \frac{1 - \tilde{x}}{\tilde{x}} \right) - (1 - 2\tilde{x})^2 \\ \hat{\omega}_s^0 &= 4(1 - \tilde{x})\tilde{x} \end{aligned} \quad (33)$$

These correspond to the “Wilson coefficients” for deep inelastic scattering, as usually calculated in the \overline{MS} scheme. It is straightforward to verify that they, indeed, are identical to the \overline{MS} Wilson coefficients.^[39] Hence, *our subtraction prescription (applicable to the general mass case) reduces to the \overline{MS} -scheme of subtraction of collinear singularities in the zero-mass limit*. This is simply a consequence of our choice of the \overline{MS} scheme to define the parton densities, which then resulted in Eq. (7) for the one-loop value of the quark density in an on-shell gluon. A change of definition of the parton densities would have added an infra-red safe term to Eq. (7), and there would be corresponding terms to be added to the other terms in the formulae we have written.

5 Results on Structure Functions

We shall now study the numerical significance of the quark scattering (QS) mechanism compared to gluon fusion (GF) in this unified framework. For the case of charged current production of a heavy quark from a light quark, we have demonstrated in a previous publication that the two basic processes are of the same size numerically; hence a quantitative QCD analysis must incorporate both in a consistent manner such as formulated above.^[30] In the following, we shall concentrate on heavy quark production by neutral current interaction which is of great interest both at fixed target and ep collider energies. For the purpose of this paper, we shall present results on the heavy quark production structure functions $F_2(x, Q)$ (which can be applied at all relevant energies). Phenomenological results on cross-sections for various interesting processes at specific energies of fixed target and HERA experiments will be pursued in a subsequent study. For practical reason, we show mostly results on charm production. At the end, we also show some corresponding results on b-production.

Two sets of parton distributions are used in the following study: the “next-to-leading order (NLO) set” consists of the CTEQ2M distributions,^[5] and the “leading order (LO) set” which is generated from initial distributions at $Q_0 = 1.6$ GeV taken from CTEQ2M but evolved using LO evolution kernel only. The differences between using LO and NLO are quite substantial, as regards the charm-quark distribution, and this is a symptom that higher order terms are important.

5.1 Scale-dependence of the Structure Function

As with all applications of the perturbative QCD parton formalism, a theoretical uncertainty about these calculations concerns the choice of factorization scale (which we identify with the renormalization scale, *cf.*, Sec. 1). Whereas some scale dependence of the theoretical prediction is unavoidable to any given order in α_s , an excessive sensitivity to the scale parameter usually signals a large theoretical uncertainty. This has been a worry for existing NLO calculations of charm and bottom production, especially for hadronic scattering.^{[25],[40]} In order to make clear how the physical results presented later might depend on the (implicit) choice of scale, we first investigate the scale dependence of the various contributions which enter our calculations. In particular, we demonstrate that whereas both the quark-scattering (QS) and the gluon-fusion (GF) terms show substantial scale dependence, these dependences are opposite in direction and they compensate each other when combined according to the variable flavor number scheme, *cf.* Eq. (9).

Fig. 7a shows $F_2(x, Q; \mu)$ as a function of μ for $x = 0.05$ and $Q = 10$ GeV, calculated using the LO parton distribution set. We display the μ -dependence of the QS (long-dashed line), the GF (dotted line), and the Subtraction (short-dashed line) terms individually along with the combined (solid line) Total result. We see that the rapid rise of the QS and the Subtraction terms together with the somewhat gentle fall of the GF contribution combine to make the Total result substantially more stable than either of the two individual production mechanisms. We also note the following important features of Fig. 7a: for μ below the heavy quark mass, the QS and subtraction terms vanish by definition (*cf.* Sec. 2.3 and Eq. (10)), we have $F_2^{Tot} = F_2^{GF}$; for μ just above the mass threshold, the QS and

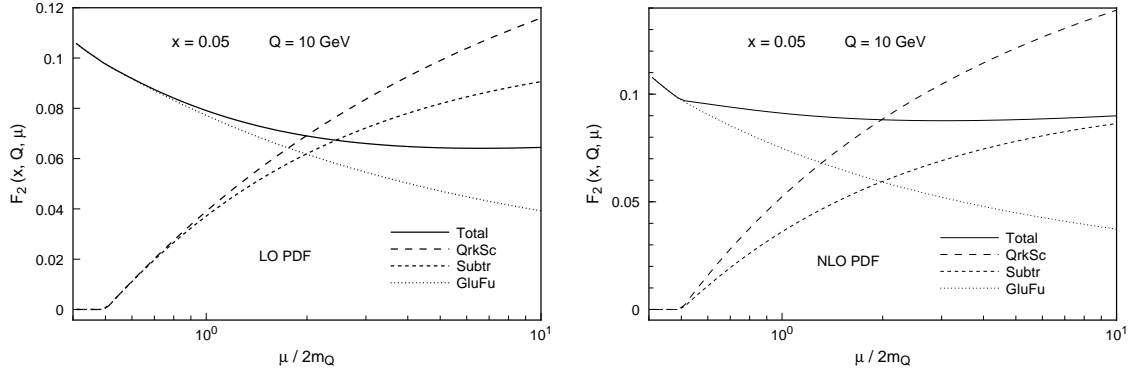


Figure 7: Scale dependence of the contributing terms to $F_2(x, Q)$. The factorization scale μ is shown in units of the physical scale $2M_Q$.

Subtraction contributions nearly cancel according to Eq. (10), we have $F_2^{Tot} \simeq F_2^{GF}$ (and the difference has reduced μ dependence); but for μ much larger than the mass threshold, Q_S (after subtraction) makes a substantial contribution to F_2^{Tot} , and F_2^{GF} ceases to be a good approximation. These features provide supporting evidence to the theoretical discussion of Sec. 2.1-2.5, as will be reinforced by results to follow.

Fig. 7b shows the corresponding results obtained with the NLO parton distribution set. All the qualitative features are the same as above. However, the cancellation between the Q_S and Subtraction terms above the heavy quark threshold is not as complete as in Fig. 7a. (The reason is that Eq. (10) is not as good an approximation as in the previous case, because the parton densities are evolved at the NLO, but Eq. (10) is only used at order α_s^1 in our calculation.) Hence the contribution of the Q_S production mechanism (after subtraction) to the structure function is even more significant for all values of μ above the threshold. The NLO parton distribution functions contain resummed sub-leading logarithms of μ/m_Q , thus the difference between the Q_S and Subtraction terms contains additional pieces of higher order terms not present in the order α_s^1 GF calculation included in this study. Note the complete stability of the Total curve against the choice of μ in this case.

These results imply that, in subsequent discussions of the x - and Q -dependencies of $F_2(x, Q)$, the choice of the scale μ can shift the Q_S , GF and Subtraction terms individually by considerable amount, but it will not affect the Total answer by nearly as much. This fact underscores the intrinsic inter-dependency of the two heavy quark production mechanisms (as a basic quantum mechanical mixing effect). It also ensures that we actually have a fair range of freedom of choice of the scale — which we can take advantage of whenever there is good physics reason to do so.

5.2 Choice of Scale

When $Q \gg m_Q$, the natural hard scale of the production process is of the order Q . For $Q \sim O(m_Q)$, μ can in principle be any combination of Q and m_Q which is of the same order of magnitude. To make an intelligent choice however, it is important to be guided by relevant physical considerations. Since we know that gluon fusion represents the correct

physics near the threshold for heavy quark production, it is appropriate to choose a μ such that the quark scattering contribution (along with the subtraction term) becomes small in this region. It also makes sense to let the latter vanish when $Q < m_Q$. As a concrete example, the following ansatz for the scale μ satisfies all these requirements.

$$\begin{aligned}\mu^2 &= m_Q^2 + c Q^2 (1 - \frac{m_Q^2}{Q^2})^n && \text{for } Q > m_Q \\ &= m_Q^2 && \text{for } Q \leq m_Q\end{aligned}\quad (34)$$

The results presented below are obtained using this ansatz with $c = 0.5$ and $n = 2$. Of course, as is the case with all pQCD calculations, an infinite number of other choices are also acceptable. However, the results of the last subsection ensure that, in our formalism, qualitative features of the answer will be common to most reasonable choices — as we have verified by actual calculation with a variety of prescriptions for μ . (This is obviously not the case if the QS or GF production mechanisms are taken individually, particularly if an extended range of Q is involved.)

5.3 Behavior of Structure Functions and the Interplay between the QS and GF Production Mechanisms

Fig. 8a shows $F_2(x, Q)$ for charm production as a function of Q for fixed $x = 0.01$ using LO parton distributions. The lines are labeled the same way as in Fig. 7. For our particular choice of scale, the QS contribution (long-dashed line) emerges from threshold and becomes comparable in size to the GF contribution (dotted line) beyond around 5 GeV. Because the subtraction term tracks the QS term rather closely throughout the kinematic range except at the very large Q end, the net contribution of these two is quite negligible, hence the Total curve (solid line) stays very close to the GF one except for very large Q .

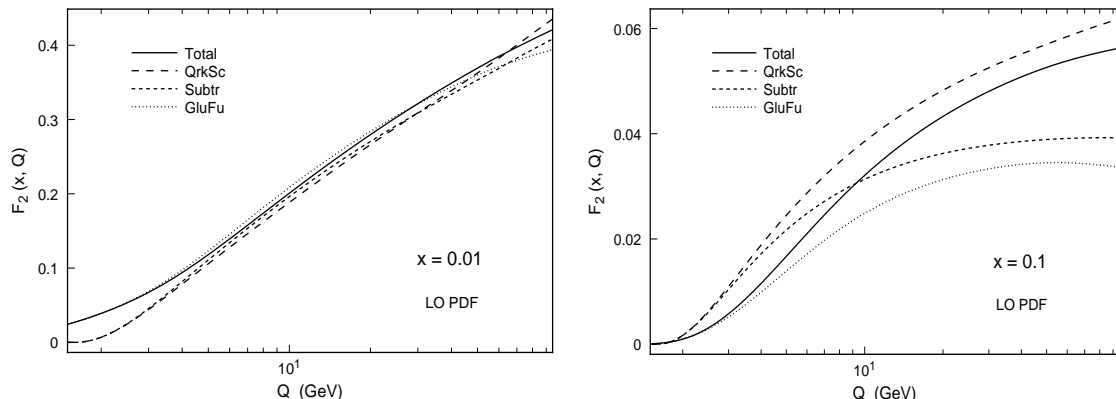


Figure 8: Q dependence of $F_2(x, Q)$ at $x = 0.01$ and $x = 0.1$ calculated using LO parton densities.

Fig. 8b is analogous to Fig. 8a except that we now look at the behavior of the various contributions to $F_2(x, Q)$ at a larger x value, $x = 0.1$. The picture is somewhat different and, for the purpose of illustrating the physics underlying our approach, more illuminating. For the same choice of scale as above, the QS contribution rises rather steeply, and overtakes

the GF contribution almost immediately above threshold. Of special interest is the behavior of the subtraction term (short-dashed line): it tracks the QS contribution above threshold, as noted before, then turns to follow the GF curve at large Q . The latter behavior follows from the definition of the subtraction as the leading collinear log term of the (order α_s) GF contribution, *cf.* Sec. 2.5 and Sec. 4.1. As a result, *the complete QCD result (the “Total” curve) follows the GF term at low Q , but it approaches the QS contribution at high Q .* We note, this same behavior is also present in Fig. 8a, for $x = 0.01$. However, there it is obscured by the closeness of the QS and GF terms due to our particular choice of scale and parton distributions.

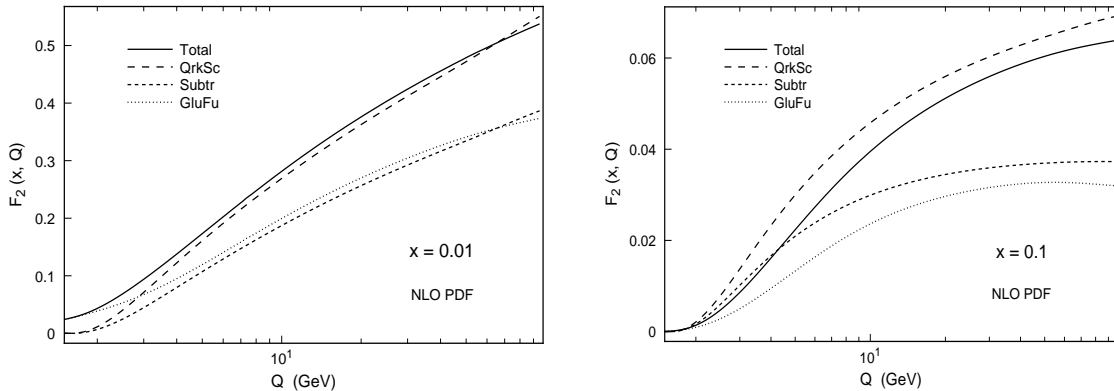


Figure 9: Q dependence of $F_2(x, Q)$ at $x = 0.01$ and $x = 0.1$ calculated using NLO parton densities.

In Figs. 9a and 9b, we show the same curves as in Figs. 8a and 8b respectively, now calculated using NLO parton distributions. The same physics effects are clearly displayed in both cases, only in more dramatic proportions.

The general feature of *close interplay between QS and GF production mechanisms* follows directly from our basic premises discussed in the introductory sections, Sec. 1 and Sec. 2: when the relevant physical energy scale (Q) is comparable to the mass of the heavy quark (m_Q), this quark behaves more like a heavy particle rather than a parton, hence GF is the dominant production mechanism,¹³ but when $Q \gg m_Q$, it behaves characteristically like a light quark parton almost by definition, and QS becomes the dominant process. This intuitively reasonable behavior naturally emerges from the *variable (scale-dependent) flavor-number scheme* of calculating massive quark production, Eq. (9).

We now look at $F_2(x, Q)$ as a function of x at fixed Q . Figs. 10a and b show the various terms for $Q = 10$ GeV calculated using LO and NLO parton distributions respectively. We see the characteristic rise of the structure function toward small x . For fixed Q , the large x limit corresponds to the total final-state energy $W \rightarrow W_{\text{threshold}}$ (for heavy quark production); all contributions become small. As $x \rightarrow 0$, one moves away from the threshold region, the relative size of the various terms are sensitive to the choice of scale and the choice of parton distribution functions.

¹³This is the basic tenet of the analysis of Collins, Soper and Sterman, Ref. [6]. The underlying physics was quantitatively demonstrated previously in a different process by Olness and Tung in Ref. [29].

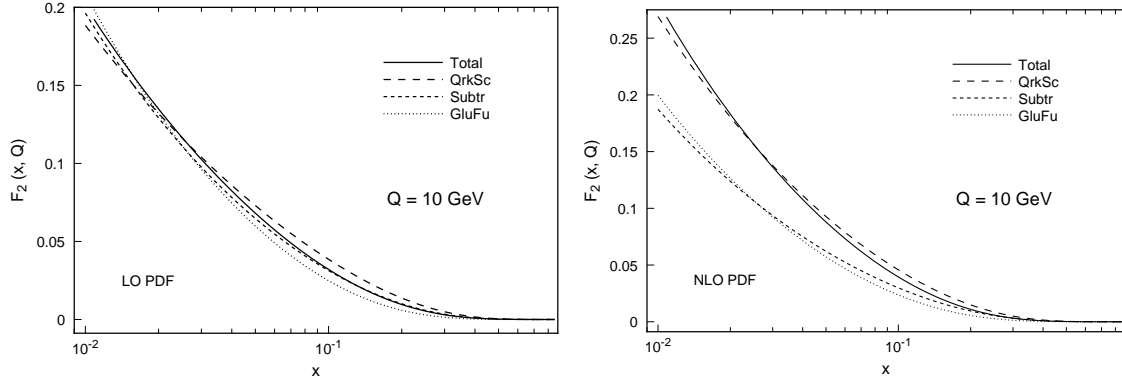


Figure 10: x dependence of $F_2(x, Q)$ at $Q = 10$ GeV calculated using LO and NLO parton densities.

These results clearly illustrate the importance of the QS (“flavor excitation” in old literature) mechanism for heavy flavor production. The GF (“flavor creation”) mechanism provides a natural explanation of the production of the heavy quarks not far above the threshold; but it is not adequate to account for this process when the energy scale becomes large. Part of the QS contribution (with proper subtraction) will be included when the next order (*i.e.*, α_s^2) GF hard-scattering terms are included.[26] However, the latter only contain terms to order $\alpha_s^2 \ln^2(\mu/M_Q)$, whereas the QS contribution represents the resummed results of all such terms to arbitrary orders.

5.4 B-quark Production

Results on b-quark production are similar to those shown for charm. We show only one plot, Fig. 11, which shows $F_2(x, Q)$ as a function of Q for fixed $x = 0.01$. We see that the features are entirely similar to those seen in Figs. 8 and 9 for charm production.

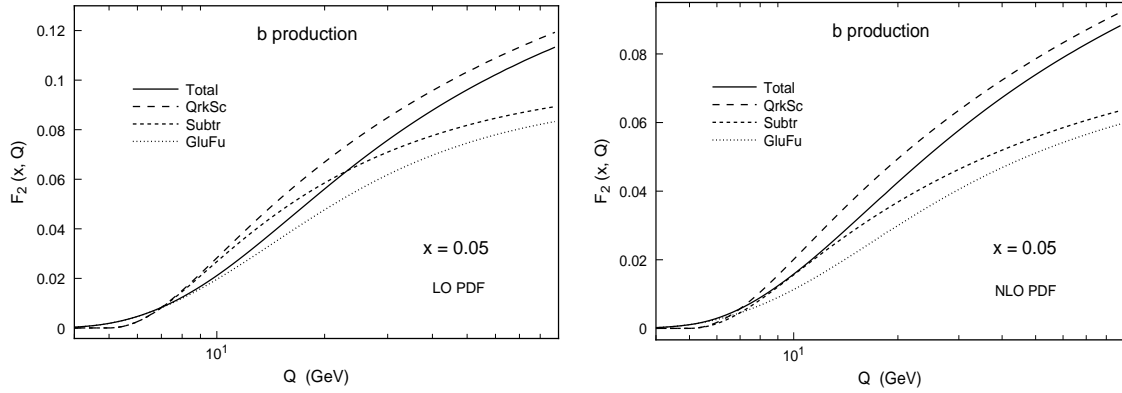


Figure 11: Structure function $F_2(x, Q)$ for b-production vs. Q at $x = 0.01$.

6 Discussions

We have shown in this paper that the currently available fixed-order QCD calculations of heavy quark production using the flavor creation mechanism alone have to be generalized to include flavor excitation with scale-dependent number of quark-flavors in order to account for the appropriate underlying physics at all energies. A consistent scheme to implement this generalization is formulated in detail to order α_s for lepton production here. The method can be extended to higher orders: in addition to the α_s^2 flavor-creation diagrams which are already calculated in the literature, one needs to add order α_s flavor-excitation (vector-boson scattering off “heavy quark” partons) contributions and perform the appropriate subtraction. As remarked earlier, these two contributions are numerically comparable in spite of the formal difference in the power of α_s by one. Exactly the same principles apply to hadroproduction. As the results of the previous section show, the inclusion of the right physics in these calculations can be expected to improve the theoretical accuracy of QCD predictions — as illustrated by the reduced dependence on the choice of (spurious) scale.

The existing fixed order calculations have a natural region of validity: when μ_{phy} is of the same order of magnitude as m_Q and x is not too small. Our proposed scheme for heavy quark production calculation contains the right physics when μ_{phy} becomes much larger than m_Q . An important question to ask is then: where exactly lies the transition region and what formalism should be used in the transition region? In order to discuss this question in specific terms, let us choose the case of charm production, ignoring b- and t-production completely.

Just above the threshold for producing charm, we all agree that fixed-order calculations using flavor creation (gluon-fusion plus light-quark scattering) alone should be reliable — *provided that the parton distribution functions used in the master formula are generated in using evolution kernels with effective flavor number $n_{eff} = 3$!* We call this method of calculation the *3-flavor scheme*. (Note, this is not usually done in the published literature. Rather, authors of the existing calculations invariably use canned parton distributions containing 4 or 5 quark-partons, depending on the energy scale. This procedure is, in principle, inconsistent.) Far above threshold, say $\mu_{phy}^2 > 20 m_Q^2$, our proposed scheme (including charm as one of the partons) should become the more reliable method. Here, we must use parton distributions generated with $n_{eff} = 4$ QCD evolution equation. We call this the *4-flavor scheme*. The question is: what scheme should be used in the transition region, say $10 m_Q^2 > \mu_{phy}^2 > 20 m_Q^2$? Although this is one of those elusive questions in pQCD which defies definitive answer, our best answer is: the region of transition should be considered as the region of co-existence of the two scheme — both schemes should be close to the real answer and either one can provide a reasonable result. For this view point to be viable, the answers obtained from the two approaches must be close to each other in the transition region, with the difference being of the order of the next order of perturbation theory, without large logarithms. The example given in the previous section indicates that indeed this is the case for some range of value of μ_{phy} . In fact, in the absence of reliable prediction of where the transition region lies (as with “when should Bjorken scaling sets in?”), the requirement of approximate equality of the prediction of the 3-flavor and 4-flavor scheme gives the most reasonable criterion for identifying where the transition takes place. (In the above discussion, we used $10 m_Q^2 > \mu_{phy}^2 > 20 m_Q^2$ only as an illustration. The appropriate

numbers should be found in this phenomenological way.)

The present paper focuses on the motivation and the physics ideas. A detailed comparison of results from the two schemes and a study of how does the transition takes place, as well as phenomenological results pertaining heavy quark production at fixed-target and collider experiments will be presented in subsequent publications.

Acknowledgement

The authors would like to thank Andrew Bazarko, Raymond Brock, Sanjib Mishra, Jorge Morfin, Michael Shaevitz, Jack Smith, and Davison Soper for useful discussions.

This work is partially supported by the National Science Foundation under Grant No.PHY89-05161, the U.S. Department of Energy Contract No. DE-FG06-85ER-40224, DE-FG05-92ER-40722, and by the Texas National Research Laboratory Commission. M.A. and F.O. also thank the Lightner-Sams Foundation for support. F.O. is supported in part by an SSC Fellowship.

References

- [1] J. Smith and W.K. Tung, in *Proceedings of 1993 Snowmass Workshop on B-Physics* MSUHEP 93/16 (to be published).
- [2] J.G. Morfin and Wu-Ki Tung, *Z. Phys.* **C52**, 13 (1991).
- [3] A. Martin *et.al.*, *Phys. Rev.*, **D45**, 2349 (1992)
- [4] J. Botts, *et al.*, *Phys. Lett.* **B304**, 159 (1993).
- [5] J. Botts, *et al.*, Preprint MSUHEP 93/18 (to be published).
- [6] J. Collins, D. Soper and G. Sterman, *Nucl. Phys.*, **B263**, 37 (1986). (This work includes a useful critique of earlier calculations of heavy quark production cross-sections in QCD.) See also: John C. Collins, D. E. Soper, G. Sterman, *Perturbative QCD*, A.H. Mueller, ed., World Scientific Publ., 1989.
- [7] E. Witten, *Nucl. Phys.*, **B104**, 445 (1976).
- [8] J. Collins, F. Wilczek, and A. Zee, *Phys. Rev.* **D18**, 242 (1978).
- [9] T. Appelquist and J. Carrazone, *Phys. Rev.* **D11**, 2856 (1975); *Nucl. Phys.* **B120**, 77 (1977); K. Symanzik, *Comm. Math. Phys.* **34**, 7 (1973).
- [10] U. Amaldi, *et al.*, *Phys. Rev.* **D36**, 1385 (1987);
See also J. Feltesse, *Proceedings of the 1989 International Symposium on Lepton and Photon Interactions at High Energies*, Stanford, August 1989, Ed. M. Riordan, p. 13, (1990).

- [11] K. Lang, *et al.*, *Z. Phys.* **C33**, 483 (1987);
 B.A. Schumm,*et al.*, *Phys. Rev. Lett.*, **60**, 1618 (1988);
 C. Foudas, *et al.*, *Phys. Rev. Lett.*, **64**, 1207 (1990);
 S.A. Rabinowitz *et al.*, *Phys. Rev. Lett.*, **70** 134 (1993);
 A. Bazarko in Proceedings of 18th Rencontres de Moriond (1993), to be published.
- [12] D. Bogert, *et al.*, *Phys. Rev. Lett.*, **55**, 1969 (1985);
Phys. Rev., **D43**, 2778 (1991);
 T. S. Mattison, *et al.*, *Phys. Rev.*, **D42**, 1311 (1990).
- [13] H. Abramowicz, *et al.*, *Phys. Rev. Lett.*, **57**, 298 (1986);
Z. Phys. **C28**, 51 (1985);
 J.P. Berge, *et al.*, *Z. Phys.* **C49**, 187 (1991).
- [14] T. Gottschalk, *Phys. Rev.* **D23**, 56 (1981).
- [15] J.J. van der Bij and G.J. van Oldenborgh, *Z. Phys.* **C51**, 477 (1991).
- [16] R.M. Barnett, *Phys. Rev. Lett.*, **36** 1163 (1976).
 R.M. Barnett, *Phys. Rev.* **D14**, 70 (1976);
 R.J.N. Phillips, *Nucl. Phys.* **B212**, 109 (1983).
- [17] R. Brock, Talk delivered at the *New Directions in Neutrino Physics at Fermilab* workshop, Batavia, Illinois, September 1988.
 R. Brock, C.N. Brown, H.E. Montgomery, M.D. Corcoran, Breckenridge Workshop, p.358, (1989), (QCD161:W638:1989).
- [18] M. Arneodo, *et al.*, *Z. Phys.* **C35**, 1 (1987);
Nucl. Phys. **B333**, 1 (1990);
Nucl. Phys. **B321**, 541 (1989);
 J.J. Aubert,*et al.*, *Phys. Lett.* **94B**, 101 (1980);
Phys. Lett. **167B**, 127 (1986);
Nucl. Phys. **B293**, 740 (1987);
- [19] J.V. Allaby, *et al.*, *Z. Phys.* **C36**, 611 (1987);
Phys. Lett. **197B**, 281 (1987);
Phys. Lett. **B213**, 554 (1988).
- [20] A. Ali, F. Barreiro, J.F. de Troconiz, G.A. Schuler, and J.J. van der Bij, Workshop on Large Hadron Colliders, Aachen, Germany, Oct 4-9, 1990. CERN report 90-10, p.917 (1990);
 A. Ali, G. Ingelman, G.A. Schuler, F. Barreiro, M.A. Garcia, J.F. de Troconiz, R.A. Eichler, and Z. Kunszt, DESY HERA Workshop (QCD161:H15:1987) p. 395, (1987).
 A. Ali in *Physics at LEP*, CERN Report 86-02, eds. J. Ellis and R. Peccei, vol.2, p.81.
- [21] G. Ingelman and G.A. Schuler, *Z. Phys.* **C40**, 299 (1988);
 Gerhard A. Schuler, *Nucl. Phys.* **B299**, 21 (1988).

[22] M. Gluck, E. Reya, M. Stratmann, DO-TH-93-20, Aug 1993.
 E. Reya, P. Zerwas, W. Hollik, V. Khoze, R.J.N. Phillips, F. Berends, D. Rein and J. Zunft, *et al.*, Proceedings of the *European Committee for Future Accelerators “Large Hadron Collider Workshop”*, CERN 90-10, eds. G.Jarlskog and D.Rein, vol.2, p.295.
 M. Glück in *Proceedings of the HERA Workshop*, Hamburg. Oct. 1987 ed. R.D Peccei, vol 1, p.119;
 M. Glück, R.M. Godbole and E.Reya, *Z. Phys.* **C38**, 441 (1988).
 M. Glück, J.F. Owens and E. Reya, *Phys. Rev.* **D17**, 2324 (1978)

[23] B. Lampe, *Z. Phys.* **C34**, 523 (1987);
 G. Kramer and B. Lampe, *Z. Phys.* **C54**, 139 (1992).

[24] Joseph F. Owens and Wu-Ki Tung, *Ann. Rev. Nucl. Part. Sci.* (1992).

[25] P. Nason, S. Dawson and R.K. Ellis, *Nucl. Phys.* **B303**, 607 (1988); **B327**, 49 (1989); (E).**B335**, 260 (1990);
 S. Frixione *et.al.*, *Phys. Lett.* **B308**, 137 (1993) and CERN-TH.6921/93.

[26] E. Laenen, S. Riemersma, J. Smith and W.L. van Neerven, *Phys. Letts.* **B291**; *Nucl. Phys.* **B392**, 162, 229 (1993).
 J. Smith and W.L. van Neerven, *Nucl. Phys.* **B374**, 36 (1992);
 S. Riemersma, J. Smith, and W.L. van Neerven, *Phys. Lett.* **B282**, 171 (1992);
 E. Laenen, J. Smith, and W.L. van Neerven, *Nucl. Phys.* **B369**, 543 (1992);
 W. Beenakker, W.L. van Neerven, R. Meng, G.A. Schuler, and J. Smith, *Nucl. Phys.* **B351**, 507 (1991);
 W. Beenakker, H. Kuijf, W.L. van Neerven, and J. Smith, *Phys. Rev.* **D40**, 54 (1989).

[27] W.J. Marciano, *Phys. Rev.* **D29** 580, (1984).

[28] J.C. Collins, W.-K. Tung *Nucl. Phys.* **B278**, 934 (1986).

[29] F.I. Olness and W.-K. Tung, *Nucl. Phys.* **B308**, 813 (1988).

[30] M.A.G. Aivazis, Fredrick I. Olness, and Wu-Ki Tung, *Phys .Rev. Lett.* **65**, 2339 (1990).

[31] M.A.G. Aivazis, Fredrick I. Olness, and Wu-Ki Tung, “Leptoproduction of Heavy Quarks I – General Formalism and Kinematics of Charged and Neutral Current Processes”, Preprint SMU-HEP/93-16, MSUHEP 93-15. Referred to as I in the text.

[32] E.M. Levin, M.G. Ryskin, Yu.M. Shabelskii, and A.G. Shuvaev, DESY-91-054;
 E.M. Levin, M.G. Ryskin, and Yu.M. Shabelskii, *Phys. Lett.* **B260**, (1991) 429.

[33] R.K. Ellis and D.A. Ross, *Nucl. Phys.* **B345**, 79 (1990);
 J.C. Collins and R.K. Ellis, *Nucl. Phys.* **B360**, 3 (1991).

[34] S. Catani, M. Ciafaloni and F. Hauptmann, *Phys. Lett.* **B242**, 97 (1990); *Nucl. Phys.* **B366** (1991) 135; also in *Proceedings of the Workshop on Physics at HERA*, Oct. 1991. eds. W. Buchmüller and G. Ingelman.

- [35] B.R. Webber, Workshop on Physics at HERA, Hamburg, Germany, Oct 29-30, 1991. DESY HERA Workshop 285, (1991) (QCD161:H51:1991);
 B.R. Webber, DESY Topical Mtg. on Small x Behavior of Deep Inelastic Structure Functions in QCD, Hamburg, Germany, May 14-16, 1990. *Nuclear Physics B Proc. Suppl.* **18C**, 38 (1991);
 J. Bartels, K. Charchula, J. Feltesse, DESY HERA Workshop 193, (1991) (QCD161:H51:1991).
- [36] M. Glück, E. Reya and M. Stratmann “Heavy Quarks at High Energy Colliders”, Dortmund preprint DO-TH 93/20.
- [37] Sijin Qian, *The CWZ subtraction scheme (A new renormalization prescription for QCD) and its applications*, Illinois Inst. of Tech. Ph.D. thesis, UMI-85-17585-mc (microfiche), May 1985.
- [38] G. Rodrigo and A. Santamaria, *Phys. Lett.* **B313**, 441 (1993).
- [39] See, for instance, W. Furmanski and R. Petronzio, *Z. Phys. C*, **11**, 293 (1982).
- [40] G. Altarelli, M. Diemoz, G. Martinelli, and P. Nason, *Nucl. Phys.* **B308**, 724 (1988).
- [41] J.C. Collins, Proc. of 25th Rencontre de Moriond: High Energy Hadronic Interactions, Les Arcs, France, Mar 11-17, p. 123 (1990).